



UNIVERSITY OF LEEDS

This is a repository copy of *High-performance symmetric supercapacitor based on new functionalized graphene oxide composites with pyrimidine nucleotide and nucleoside*.

White Rose Research Online URL for this paper:

<https://eprints.whiterose.ac.uk/182006/>

Version: Supplemental Material

Article:

Dashti Najafi, M, Kowsari, E, Reza Naderi, H et al. (5 more authors) (2022) High-performance symmetric supercapacitor based on new functionalized graphene oxide composites with pyrimidine nucleotide and nucleoside. *Journal of Molecular Liquids*. 118381. ISSN 0167-7322

<https://doi.org/10.1016/j.molliq.2021.118381>

© 2021, Elsevier. This manuscript version is made available under the CC-BY-NC-ND 4.0 license <http://creativecommons.org/licenses/by-nc-nd/4.0/>.

Reuse

This article is distributed under the terms of the Creative Commons Attribution-NonCommercial-NoDerivs (CC BY-NC-ND) licence. This licence only allows you to download this work and share it with others as long as you credit the authors, but you can't change the article in any way or use it commercially. More information and the full terms of the licence here: <https://creativecommons.org/licenses/>

Takedown

If you consider content in White Rose Research Online to be in breach of UK law, please notify us by emailing eprints@whiterose.ac.uk including the URL of the record and the reason for the withdrawal request.



eprints@whiterose.ac.uk
<https://eprints.whiterose.ac.uk/>

Supporting Information

High-performance symmetric supercapacitor based on new functionalized graphene oxide composites with pyrimidine nucleotide and nucleoside

Mohammad Dashti Najafi ^a, Elaheh Kowsari ^{a, 1*}, Hamid Reza Naderi ^b, Saeedeh Sarabadani Tafreshi ^a, Amutha Chinnappan ^c, Seeram Ramakrishna ^{c, *}, Nora H. de Leeuw ^{d,e}, Ali Ehsani ^f

^a Department of Chemistry, Amirkabir University of Technology, No. 424, Hafez Avenue, 1591634311, Tehran, Iran

^b Novin Ebtekar Company, Exclusive Agent of Metrohm-Autolab and Dropsens Companies, Tehran, Iran

^c Department of Mechanical Engineering, Center for Nanofibers and Nanotechnology, National University of Singapore, Singapore

^d School of Chemistry, Cardiff University, Main Building, Park Place, Cardiff CF10 3AT, United Kingdom

^e now at: School of Chemistry, University of Leeds, Leeds LS2 9JT, United Kingdom

^f Department of Chemistry, Faculty of science, University of Qom, Qom, Iran

¹* corresponding authors

E-mail addresses: Kowsarie@aut.ac.ir (E. Kowsari) and seeram@nus.edu.sg (S. Ramakrishna)

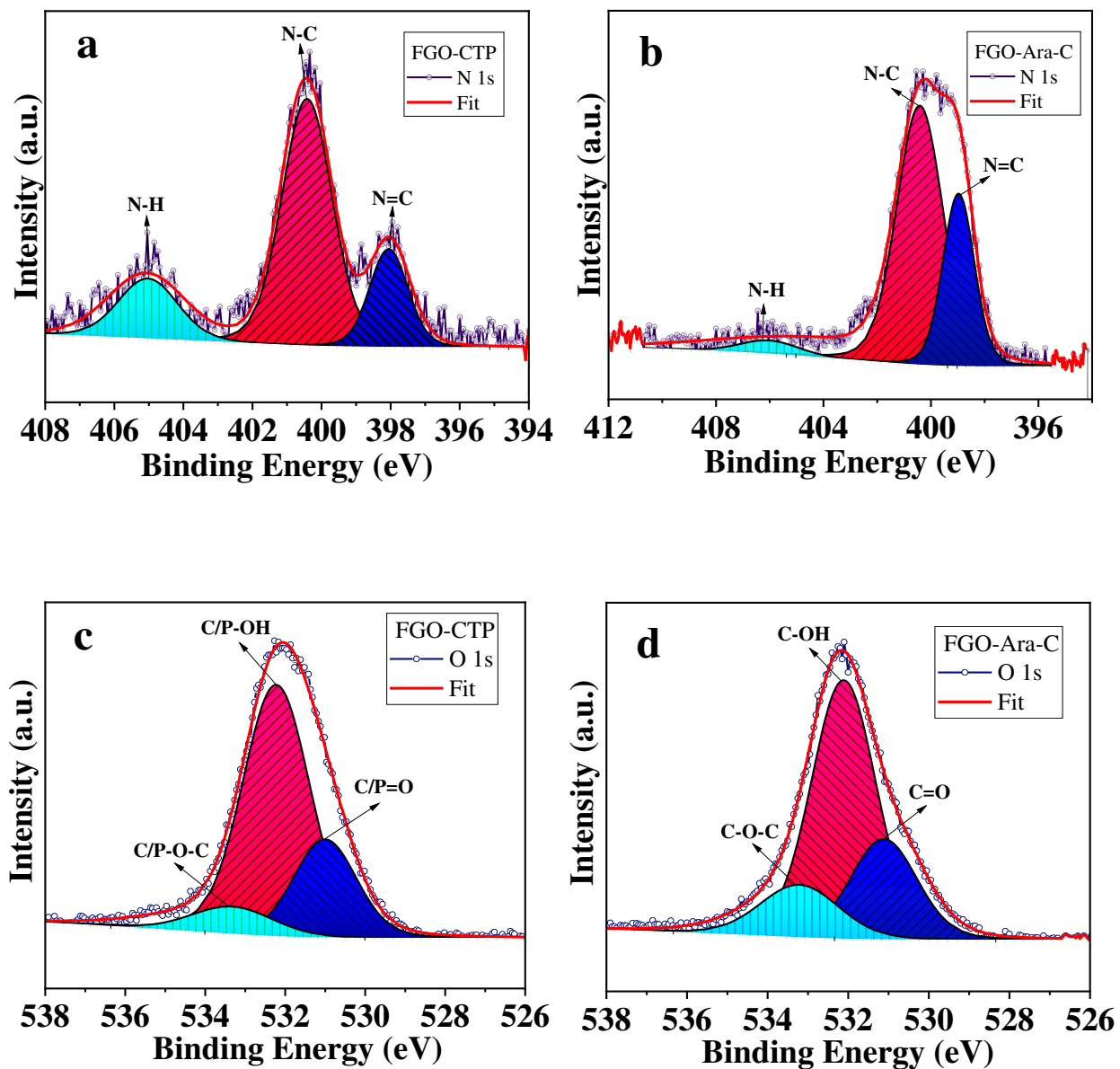
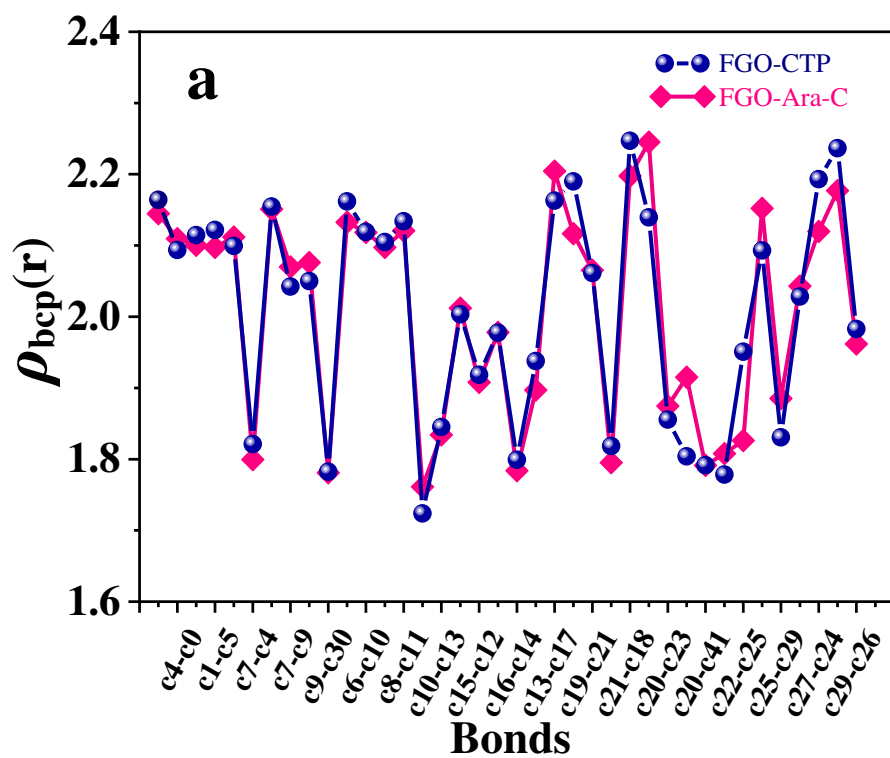


Fig. S1. XPS spectra of N 1s of as-synthesized (a) FGO-CTP and (b) FGO-Ara-C; Core level spectrum of O 1s as-synthesized (c) FGO-CTP and (d) FGO-Ara-C.

Table. S1. BET specific surface area, Total pore volume, BJH pore volume, BJH pore size, and average pore size of GO, FGO-CTP, and FGO-Ara-C.

	BET surface area (m ² g ⁻¹)	Total pore volume (cm ³ g ⁻¹)	BJH pore volume (cm ³ g ⁻¹)	BJH pore size (nm)	Average pore size (nm)
GO	24.188	0.026	0.018	1.213	4.268
FGO-Ara-C	33.759	0.072	0.049	1.213	8.511
FGO-CTP	45.551	0.093	0.066	1.215	10.998



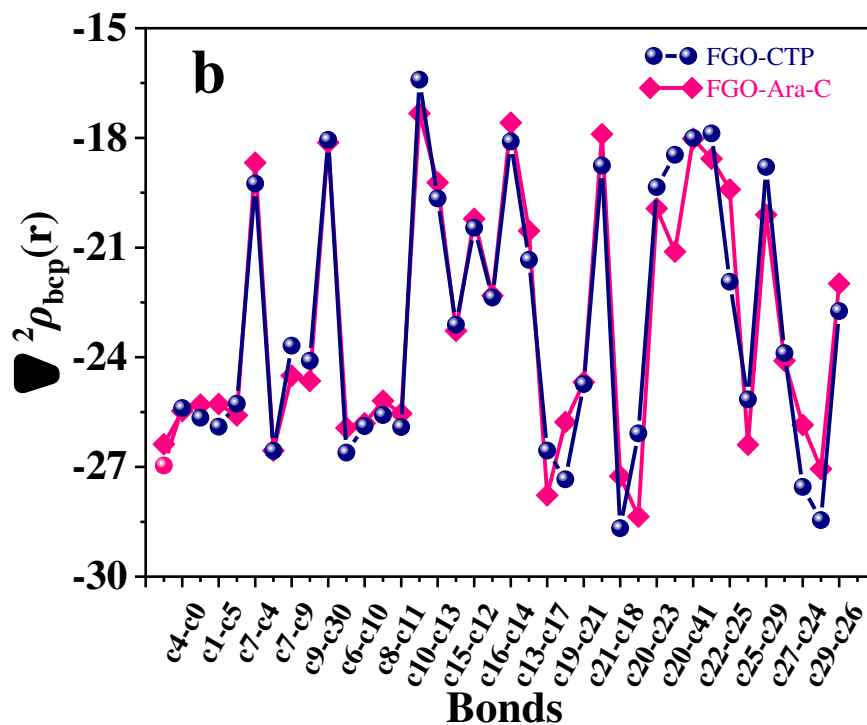


Fig. S2. The differences of (a) electron density $\rho_{bcp}(r)$ and (b) the Laplacian of electron density $\nabla^2\rho_{bcp}(r)$ of carbon atoms of GO layer of FGO-Ara-C and FGO-CTP complexes.

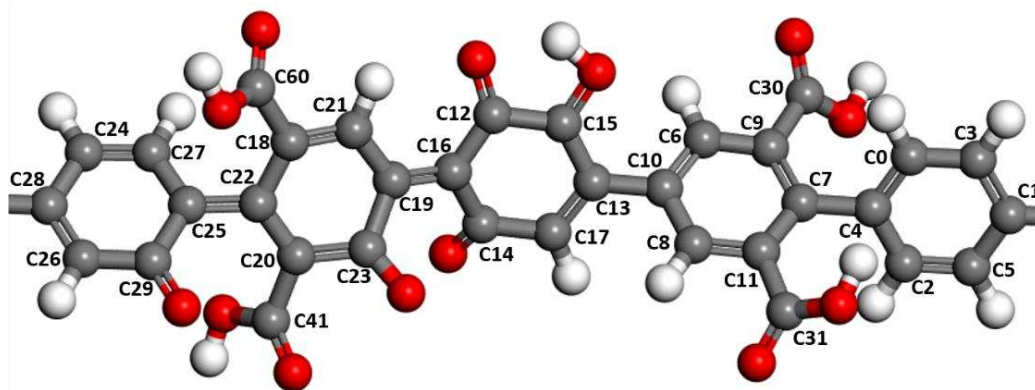


Fig. S3. The ball and stick model of GO layer used in the DFT calculation.

Table S2. The topological properties of electron density of carbon bonds on GO layer of FGO-Ara-C and FGO-CTP complexes obtained from DFT calculations. For finding the Carbon atoms refer to the Fig. S3.

Bonds	FGO-Ara-C	FGO-Ara-C	FGO-CTP	FGO-CTP
	$\rho_{\text{bcp}}(\mathbf{r})$	$\nabla^2\rho_{\text{bcp}}(\mathbf{r})$	$\rho_{\text{bcp}}(\mathbf{r})$	$\nabla^2\rho_{\text{bcp}}(\mathbf{r})$
C0-C3	2.145	-26.379	2.164	-26.959
C0-C4	2.109	-25.471	2.094	-25.391
C1-C3	2.100	-25.299	2.114	-25.652
C1-C5	2.097	-25.280	2.122	-25.899
C2-C4	2.112	-25.589	2.099	-25.271
C4-C7	1.799	-18.680	1.821	-19.247
C2-C5	2.151	-26.552	2.155	-26.559
C7-C9	2.070	-24.504	2.042	-23.682
C7-C11	2.076	-24.649	2.050	-24.095
C9-C30	1.781	-18.127	1.782	-18.058
C6-C9	2.133	-25.935	2.162	-26.610
C10-C6	2.118	-25.808	2.119	-25.885
C8-C10	2.097	-25.190	2.105	-25.583
C8-C11	2.121	-25.540	2.134	-25.909
C11-C31	1.761	-17.331	1.724	-16.409
C10-C13	1.834	-19.223	1.845	-19.656
C13-C15	2.012	-23.275	2.003	-23.110
C12-C15	1.908	-20.210	1.918	-20.457
C12-C16	1.978	-22.313	1.978	-22.363
C14-C16	1.784	-17.584	1.799	-18.097
C14-C17	1.897	-20.543	1.938	-21.337
C13-C17	2.204	-27.774	2.163	-26.552
C16-C19	2.117	-25.771	2.190	-27.337
C19-C21	2.065	-24.681	2.061	-24.734
C19-C23	1.795	-17.899	1.818	-18.758
C18-C21	2.198	-27.255	2.247	-28.674
C20-C20	2.245	-28.359	2.139	-26.084
C20-C23	1.875	-19.933	1.856	-19.348
C18-C22	1.915	-21.111	1.804	-18.465
C20-C41	1.791	-18.023	1.792	-18.001
C18-C60	1.808	-18.569	1.778	-17.879
C22-C25	1.826	-19.410	1.951	-21.935
C25-C27	2.152	-26.394	2.093	-25.155
C25-C29	1.885	-20.102	1.831	-18.793
C24-C28	2.043	-24.095	2.028	-23.886
C24-C27	2.120	-25.855	2.193	-27.546
C26-C28	2.177	-27.056	2.237	-28.453
C26-C29	1.962	-21.985	1.983	-22.738

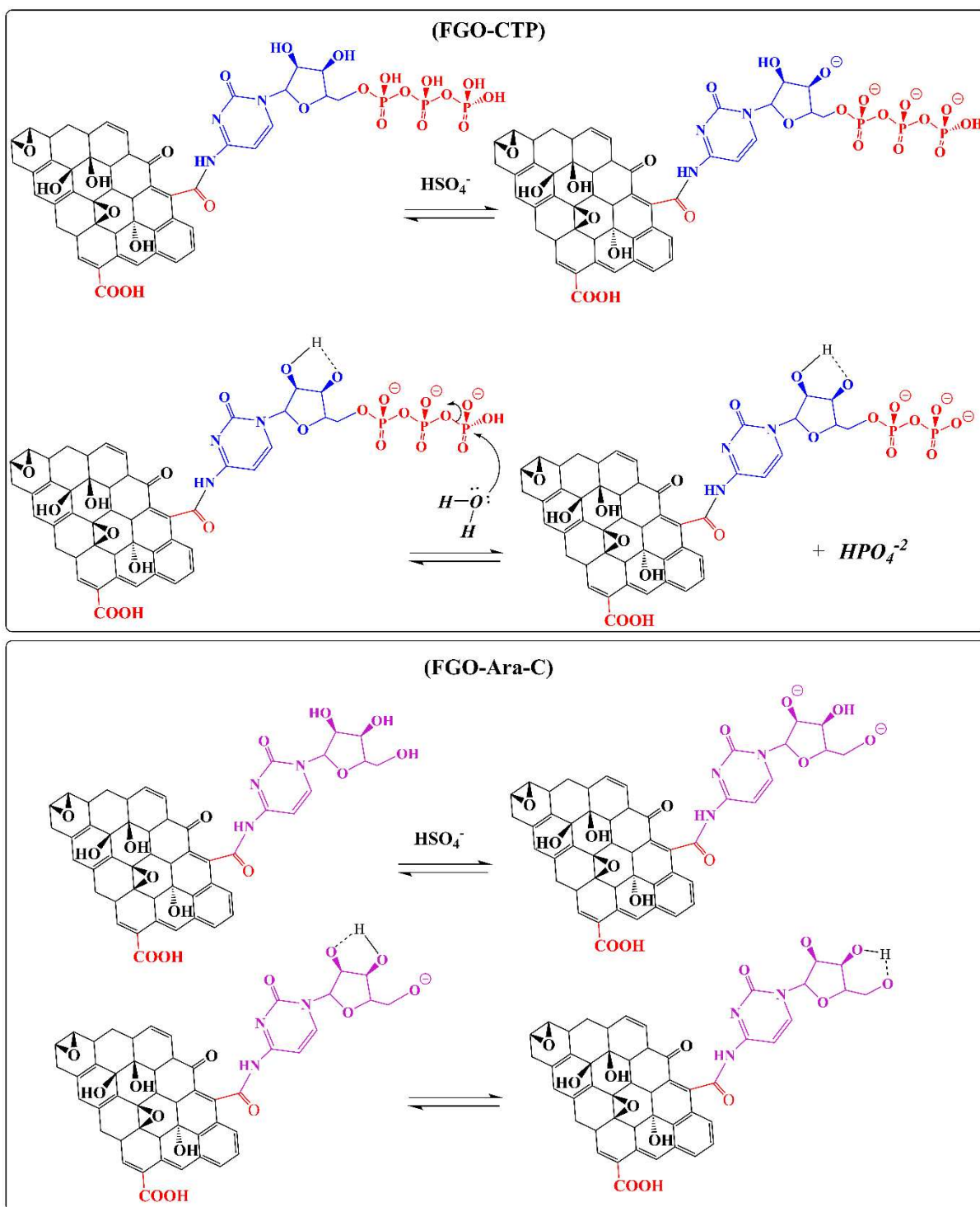


Fig. S4. Mechanism of redox reactions of FGO-CTP and FGO-Ara-C.

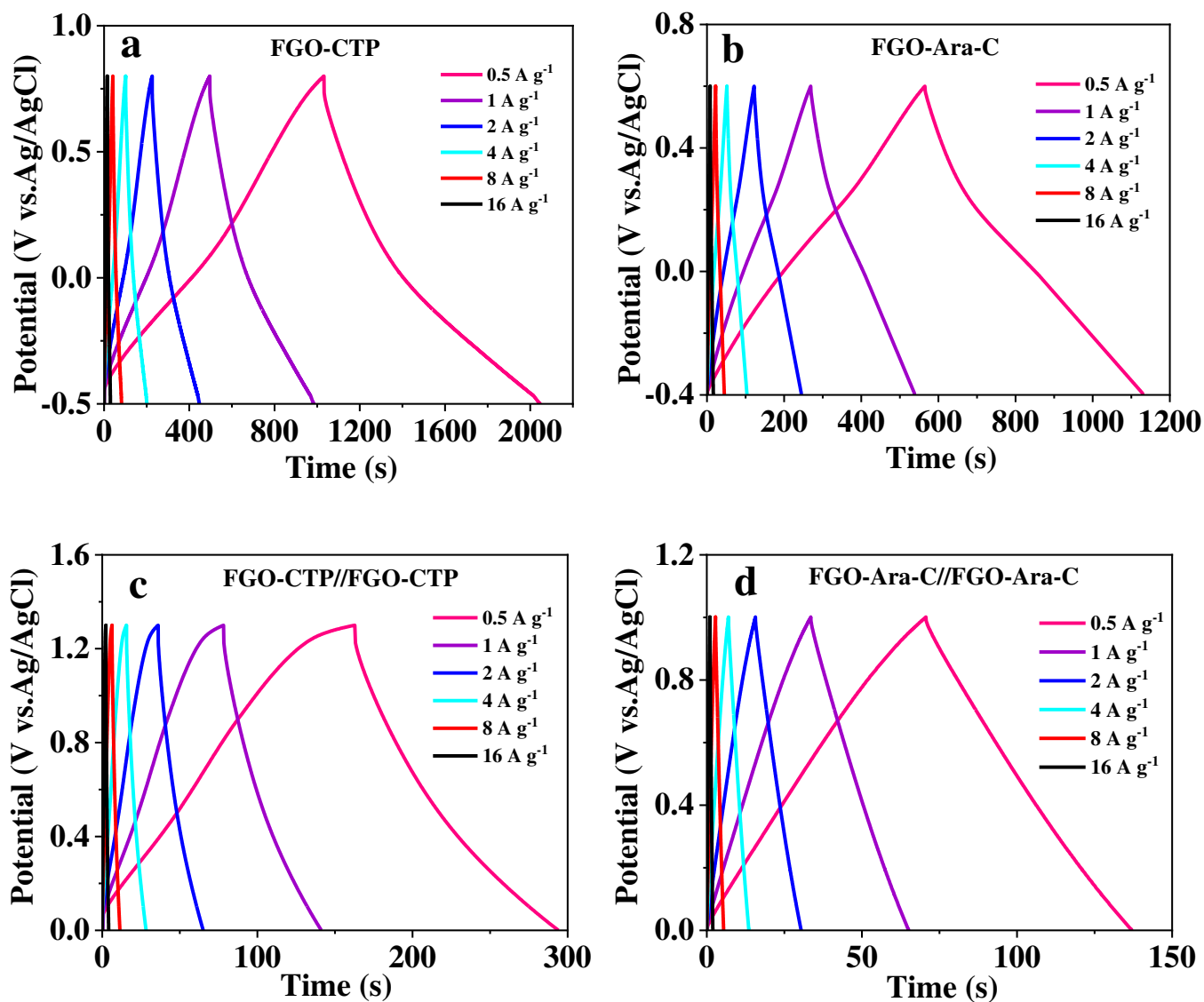


Fig. S5. GCD curves of (a) FGO-CTP, (b) FGO-Ara-C, (c) FGO-CTP//FGO-CTP, and (d) FGO-Ara-C//FGO-Ara-C at the current densities rates of 0.5-16 A g⁻¹.